Published OnlineFirst December 8, 2009; DOI: 10.1158/0008-5472.CAN-09-3324

Cancer Research

A Gold(III) Porphyrin Complex with Antitumor Properties Targets the Wnt/β-catenin Pathway

Kim Hei-Man Chow[1,2,3], Raymond Wai-Yin Sun[1], Janice B.B. Lam[1,2,3], Carrie Ka-Lei Li[1], Aimin Xu[2,3], Dik-Lung Ma[1], Ruben Abagyan[4], Yu Wang[1,2], and Chi-Ming Che[1]

Abstract

Gold(III) complexes have shown promise as antitumor agents, but their clinical usefulness has been limited by their poor stability under physiological conditions. A novel gold(III) porphyrin complex [5-hydroxyphenyl-10,15,20-triphenylporphyrinato gold(III) chloride (gold-2a)] with improved aqueous stability showed 100-fold to 3,000-fold higher cytotoxicity than platinum-based cisplatin and IC_{50} values in the nanomolar range in a panel of human breast cancer cell lines. Intraductal injections of gold-2a significantly suppressed mammary tumor growth in nude mice. These effects are attributed, in part, to attenuation of Wnt/β-catenin signaling through inhibition of class I histone deacetylase (HDAC) activity. These data, in combination with computer modeling, suggest that gold-2a may represent a promising class of anticancer HDAC inhibitor preferentially targeting tumor cells with aberrant Wnt/β-catenin signaling. *Cancer Res; 70(1); 329–37. ©2010 AACR.*

Introduction

Breast cancer represents the most common diagnosed female malignancy and the second leading cause of women death worldwide (1). Chemotherapeutic agents are commonly used and usually given in the form of combinational chemotherapy (2). However, the effects of these agents are not universal, and a large portion of patients will develop resistance. Moreover, side effects including induction of life-threatening toxicity are commonly encountered.

Therapeutic values of gold have been recognized thousands of years ago, and its rational use in medicine began in early 1920s (3–7). Because gold(III) is isoelectronic with platinum (II) and tetracoordinate gold(III) complexes are in the same square-planar geometries as cisplatin, the potential anticancer properties of gold(III) complexes have been investigated for almost three decades (8, 9). A number of gold(III) complexes have been reported to exhibit cytotoxicities against a broad spectrum of tumor cells, and their potencies (IC_{50} values in low micromolar range) are comparable with that of cisplatin. In contrast to general expectations, evidence suggest that the gold(III) complexes exert their antiproliferative activities through mechanisms that are substantially different from those of platinum drugs (10). Yet, the molecular mechanisms and targets of gold(III)-based antitumor metallodrugs remain largely uncharacterized.

Previously we synthesized a series of gold(III) *meso*-tetraarylporphyrin complexes characterized by enhanced stability in aqueous solutions and under physiological conditions (11). Among them, gold-1a [5,10,15,20-tetraphenylporphyrinato gold(III) chloride] showed promising antiproliferative activities against human cancer cells, including those derived from neuroblastoma, colon, nasopharyngeal, and hepatocellular carcinomas (11–15). In the present study, a novel gold(III) porphyrin analogue [5-hydroxyphenyl-10,15,20-triphenylporphyrinato gold(III) chloride (gold-2a)] was prepared by modifying one of the peripheral phenyl groups of the gold-1a with a hydroxyl substitution to improve its aqueous solubility (Supplementary Fig. S1). The efficacy of gold-2a in suppressing the growth of a panel of human breast cancer cells was evaluated *in vitro*, and its anticancer activity was investigated in nude mice. Our results suggest that gold-2a is a promising drug lead for anti–breast cancer treatment and that it can selectively inhibit Wnt/β-catenin signaling through modulating histone deacetylase (HDAC) activities.

Materials and Methods

Preparation of gold(III) porphyrin complex (gold-2a). The synthesis of the gold(III) porphyrin complex (gold-2a) was conducted under a nitrogen atmosphere using the standard Schlenk technique (11). ^1H nuclear magnetic resonance (NMR) spectrum was recorded on a DPX-400 Bruker FT-NMR spectrometer with chemical shift (in ppm) relative to tetramethylsilane. Absorption spectrum was recorded on a Perkin-Elmer Lambda 900 UV-vis spectrophotometer. Mass spectrum (FAB) was recorded on a Finnigan MAT95 mass

Authors' Affiliations: [1]Department of Chemistry and Open Laboratory of Chemical Biology of the Institute of Molecular Technology for Drug Discovery and Synthesis, Departments of [2]Pharmacology and Pharmacy and [3]Medicine, The University of Hong Kong, Pokfulam, Hong Kong, China; and [4]Skaggs School of Pharmacy and Pharmaceutical Sciences, University of California, San Diego, La Jolla, California

Note: Supplementary data for this article are available at Clinical Cancer Research Online (http://clincancerres.aacrjournals.org/).

K.H-M. Chow and R.W-Y. Sun contributed equally to this work.

Corresponding Author: Yu Wang, Department of Pharmacology and Pharmacy, Faculty of Medicine Building, 21 Sassoon Road, Pokfulam, Hong Kong. Phone: 852-28192864; Fax: 852-28170859; E-mail: yuwanghk@hku.hk or Chi-Ming Che, Department of Chemistry, the University of Hong Kong, Pokfulam Road, Hong Kong. Phone: 852-28592154; Fax: 852-29155176; E-mail: cmche@hku.hk.

doi: 10.1158/0008-5472.CAN-09-3324

Published OnlineFirst December 8, 2009; DOI: 10.1158/0008-5472.CAN-09-3324

spectrometer using 3-nitrobenzyl alcohol (NBA) as the matrix. Elemental analyses were performed at the Institute of Chemistry at Chinese Academy of Sciences, Beijing. The gold-2a was obtained at a yield of 77%. ^{1}H NMR ($CDCl_3$): δ = 9.44 (d, J = 5.2 Hz, 2H), 9.30–9.25 (m, 6H), 8.23 (d, J = 6.3 Hz, 6H), 7.93-7.79 (m, 11H), 7.32 (d, J = 8.4 Hz, 2H). UV-vis (DMSO) λ_{max}/nm (log ε): 414 (5.35), 526 (4.30). FAB-MS: m/z 826 [M^+]; elemental analysis calculated (%) for $C_{44}H_{28}N_4OClAu$: C, 61.37; H, 3.28; N, 6.51. Found: C, 61.54; H, 3.17; N, 6.46. For cell culture and other *in vitro* experiments, gold-2a and cisplatin were dissolved in DMSO, whereas for *in vivo* animal administration, these complexes were dissolved in PET (a mixture of 60% polyethylene glycol, 30% ethanol, and 10% Tween-80) and further diluted with PBS at a 1:9 ratio.

Cell proliferation measurement. Cell proliferation was evaluated by crystal violet staining and [^{3}H]thymidine incorporation methods as described previously (16, 17). The human breast carcinoma BT474, MCF-7, MDA-MB-231, SKBR3, T47D cell lines were obtained from American Type Culture Collection on December 2004. The identities of these cells were confirmed by STR-profiling using the Cell ID System from Promega (last tested on 16/02/09).

Inoculation of breast cancer cells into nude mice and drug treatment. MDA-MB-231 cells (5×10^6) were implanted into the third right thoracic mammary fat pad of female nude mice (6 wk old) as described before (17). Six days after the implantation, the mice were divided into groups consisting of animals bearing almost the same size of tumor. Intraductal administration of the drugs was performed at the 7th and 11th days after initial implantation (day 0). I.p. drug administration was performed twice weekly as indicated. Tumor development was monitored every 3 to 4 d using digital vernier calipers, with tumor volume calculated using the formula [sagittal dimension (mm) × cross-dimension (mm)]^2 / 2 and expressed in mm^3. All animal experimental protocols were approved by the animal ethics committee at the University of Hong Kong.

β-Catenin/T-cell factor-lymphoid enhancer factor-1 transcription reporter assay. Nuclear activities of endogenous β-catenin were analyzed by TOPflash/FOPflash reporter system (17).

Quantitative reverse transcription–PCR and chromatin immunoprecipitation–PCR. Quantitative reverse transcription–PCR (RT-PCR) was performed as described (17). The primers were listed in Supplementary Table S1. The histone acetylation at the promoter regions of different genes was compared by chromatin immunoprecipitation (ChIP)–PCR and ChIP-QPCR. Briefly, 8×10^6 tumor cells were cross-linked with 1% formaldehyde and sheared by sonication to obtain chromatin with an average DNA length of 500 to 1,000 bp. After a 3-h preclear with protein G–Sepharose beads (blocked with 0.2 mg/mL salmon sperm DNA and 0.5 mg/mL bovine serum albumin), 100 μg chromatin were incubated with 2 μg of antibodies at 4°C overnight. Immunocomplexes were collected by protein G–Sepharose (blocked as above), washed, and eluted in 50-μL elution buffer (0.1 mol/L $NaHCO_3$, 1% SDS). After reversed cross-linking, the chromatin fragments were purified by phenol-chloroform extraction. PCR amplifications were performed using 10% of the DNA samples, and the resulting products were quantified by densitometry (MultiAnalyst Software, Bio-Rad). The primers were listed in Supplementary Table S2. Quantitation was also performed using real-time PCR analysis.

HDAC activity assay. HDAC activity was determined using the colorimetric HDAC activity assay kit (BioVision, Inc.) and the Fluor de Lys Substrate (BML-AK500, BIOMOL International) according to the manufacturer's instructions. Briefly, for *in vitro* HDAC activity determination, 150 μg of MDA-MB-231 nuclear extracts were incubated with different dosages of gold-2a for various periods of time. The reaction was initiated by addition of HDAC colorimetric substrate and incubation at 37°C for 1 h. The developer was then added, and the samples were incubated at 37°C for another 30 min before reading at 405 nm. Cells pretreated with drug compounds were also processed for HDAC activity measurement. In addition, the inhibitory effects of gold-2a on individual HDACs were tested using immunoprecipitated complexes.

Histone acetylation analysis. Histones were extracted according to the procedure reported previously (18). The acid soluble histone fraction was subjected to 18% SDS-PAGE and Western blotting analysis.

Inductively coupled plasma–mass spectrometry analysis. Subcellular fractionation was performed as described (19). Nuclear fractions were further separated into nuclear matrix, nucleoid, and nucleolus. All samples were subjected to inductively coupled plasma–mass spectrometry (ICP-MS) analysis (7500 series, Agilent Technologies, Inc.) for determining the content of the stable gold isotope ^{197}Au (20).

Molecular docking. The 1.9-Å X-ray structure of HDAC8 (Protein Data Bank code 1t64) was used for docking calculations using Gaussian 03. The gold-2a complex was optimized using DFT with a LanL2MB basis set (21). ICM-Pro 3.6-1 program (Molsoft) was applied for molecular docking. Energy calculations were based on the ECEPP/3 force field with a distance-dependent dielectric constant (22). The biased probability Monte Carlo minimization procedure was used for global energy optimization. All ICM dockings were performed thrice, and a minimum of the three interaction energies was used.

Data analysis and statistics. All experiments were performed with three to eight samples per group, and all results were derived from at least three independent experiments. Data are shown as mean values ± SD. Unless otherwise specified, comparison between groups was done using Student's t test. $P < 0.05$ was used to indicate a significant difference.

Results

Gold-2a exerts potent antiproliferative activities against human breast cancer cells. Five types of human breast carcinoma cells with distinct gene expression profiles and oncogenic phenotypes, including BT474, MCF-7, T47D, MDA-MB-231, and SKBR3 (23), were used for evaluating the cytotoxicity of gold-2a. Crystal violet assay showed that gold-2a inhibited growth of all five types of cells at mean IC_{50} values of 0.49 ± 0.17, 0.08 ± 0.04,

Published OnlineFirst December 8, 2009; DOI: 10.1158/0008-5472.CAN-09-3324

Table 1. Antiproliferative activities of gold-2a and cisplatin in various human breast carcinoma cells

Drug	Period of treatment (h)	Conditions	IC_{50} (μmol/L)				
			BT474	MCF7	MDA-MB-231	SKBR3	T47D
Gold-2a	24	0.5% FBS	0.49 ± 0.17	0.08 ± 0.04	0.007 ± 0.002	0.02 ± 0.01	0.04 ± 0.01
		10% FBS	0.39 ± 0.18	0.16 ± 0.08	0.003 ± 0.008	0.04 ± 0.02	0.06 ± 0.03
	48	0.5% FBS	0.15 ± 0.07	0.07 ± 0.04	0.004 ± 0.001	0.07 ± 0.002	0.02 ± 0.01
		10% FBS	0.12 ± 0.09	0.05 ± 0.01	0.001 ± 0.006	0.08 ± 0.01	0.05 ± 0.01
Cisplatin	24	0.5% FBS	49.0 ± 0.50	14.3 ± 1.46	7.37 ± 1.19	65.9 ± 25.5	66.5 ± 12.4
		10% FBS	45.1 ± 8.20	20.1 ± 4.92	21.0 ± 11.2	76.3 ± 33.8	99.4 ± 5.71
	48	0.5% FBS	1.60 ± 0.53	10.1 ± 1.47	6.52 ± 0.48	33.9 ± 11.0	7.76 ± 5.54
		10% FBS	2.89 ± 0.90	15.9 ± 2.33	18.4 ± 3.42	41.0 ± 7.91	6.69 ± 3.14

0.04 ± 0.01, 0.007 ± 0.002, and 0.02 ± 0.01 μmol/L, respectively [0.5% fetal bovine serum (FBS) condition, 24-hour treatment; Table 1]. The presence of high concentrations of serum had no effects on the potencies of the drug. In contrast, the IC_{50} values of cisplatin were ~100 to 3,000 times higher than gold-2a. Similar results were observed when the drug exposure time was extended to 48 hours. It should be noted that the IC_{50} values of gold-2a were one to two logs lower in MDA-MB-231 cells than the other four types of cells under all conditions. On the other hand, the potency of gold-2a toward noncancerous fibroblast cell was ~10-fold to 600-fold lower than those of mammary cancer cells with an IC_{50} of 4.17 ± 1.67 μmol/L. The antiproliferative activity of another gold(III) porphyrin complex {[Au^{III}(TPP)]Cl, gold-1a} in MDA-MB-231 cells was also tested. Nonlinear regression analysis of the growth inhibition curves revealed that gold-1a was ~450-fold less effective than gold-2a (IC_{50}, 1.351 ± 0.032 μmol/L versus 0.003 ± 0.008 μmol/L). Apoptosis of MDA-MB-231 cells were evaluated by measuring DNA fragmentation and terminal deoxynucleotidyl transferase-mediated dUTP nick end labeling analysis. The results showed that gold-2a significantly increased DNA fragmentation and the number of apoptotic cells in a dose- and time-dependent manner (Supplementary Fig. S2).

Intraductal delivery of gold-2a effectively attenuates mammary MDA-MB-231 tumor growth in nude mice. To evaluate the *in vivo* antitumor effects of gold-2a, MDA-MB-231 cells were implanted into athymic nude mice and different drug dosages were tested for the treatment. Biweekly i.p. administration of gold-2a (1.5, 3.0, and 6.0 mg/kg) for up to 4 weeks dose-dependently attenuated the tumor growth (Supplementary Fig. S3). However, no complete tumor suppression could be achieved despite the fact that the animals tolerated the treatment well. Instead, the administration of two bolus of the gold-2a (15 mg/kg) by intraductal injection into tumor xenograft resulted in a complete tumor remission in 50% of the animals at 2 weeks after initial implantation (Fig. 1*A*). Most of the animals remained in a tumor-free status until day 25, at which recurrence of tumor was observed. Comparing to gold-2a, intraductal delivery of the same dosage of cisplatin attenuated the rates of tumor growth to a much less degree. Of note is that ~40% of animals died in the cisplatin treatment group after two injections, whereas those of the PET control and gold-2a treatment groups remained alive during the experimental periods (Fig. 1*B*). The body weights of both gold-2a– and cisplatin-treated mice were slightly lower than the PET control group (Fig. 1*C*). The average tumor weights in gold-2a and cisplatin groups were 0.17 ± 0.02 and 0.42 ± 0.15 g, respectively, which were decreased by 73% and 34% when compared with control group (Fig. 1*D*).

Gold-2a inactivates Wnt/β-catenin signaling in MDA-MB-231 cells through transcriptional regulation. Aberrant activation of the Wnt/β-catenin signaling and intracellular accumulation of β-catenin protein have been observed in a large portion of human breast tumors (24, 25). Gold-2a decreased the protein levels of β-catenin in MDA-MB-231 cells as early as 4 hours after treatment (Supplementary Fig. S4*A*). Nuclear transcriptional activities of β-catenin were also dramatically reduced by gold-2a (Supplementary Fig. S4*B*). On the contrary, cisplatin had no influence on both the protein levels and nuclear activities of β-catenin. In the absence of a Wnt signal, β-catenin is phosphorylated by glycogen synthase kinase-3β, which facilitates the subsequent ubiquintination and proteasome degradation. However, gold-2a treatment did not alter the relative phosphorylation or ubiquintination levels of β-catenin and had no obvious effects on proteasome activities (Supplementary Fig. S5). In the mean time, decreased phosphorylations of Akt and GSK-3β were observed from 6 hours onward after gold-2a treatment, later than the effects on β-catenin protein levels (Supplementary Fig. S4*A*). To address the cytotoxic mechanisms of gold-2a, ICP-MS was performed for monitoring the intracellular localization of this complex. The results showed that gold-2a rapidly (within 30 min) entered the nuclei of MDA-MB-231 cells and was enriched in the nucleoid fractions (Supplementary Fig. S4*C*).

The drop in intracellular levels of β-catenin can be triggered by a loss of Wnt signal–induced stabilization (26). In fact, quantitative PCR analysis revealed that gold-2a treatment time- and dose-dependently altered the mRNA expressions of several Wnt signaling molecules, including *WNT1, WNT5B, WIF1, WISP1*, and *CTNNB1* (Fig. 2). For instance, gold-2a treatment largely blocked the expression of *WNT1* but profoundly augmented the mRNA levels of *WIF1*. Significant upregulation of *WIF1* (over 80-fold) was

Published OnlineFirst December 8, 2009; DOI: 10.1158/0008-5472.CAN-09-3324

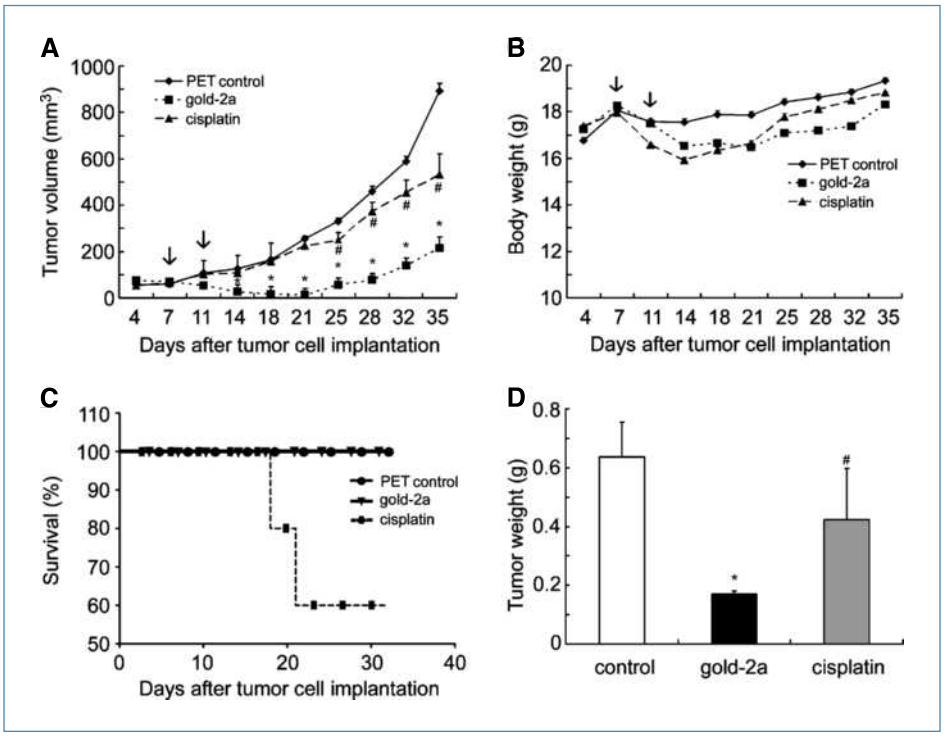

Figure 1. Gold-2a inhibits mammary tumor growth in nude mice. MDA-MB-231 cells were inoculated into the mammary fat pad of nude mice. Gold-2a, cisplatin, or PET control was locally injected into the tumor site at day 7 and day 11. Tumor growth (*A*) and body weight (*B*) were monitored semiweekly. *C*, Kaplan-Meier estimates of the survival curves were calculated and plotted. *D*, at the end of experiment, tumors were collected and weighed. # and *, $P < 0.05$ versus PET control ($n = 4–6$).

observed at as early as 2 hours, and the stimulatory effects continued during the 24-hour course of treatment. The mRNA levels of *WISP1* were rapidly decreased to an undetectable level after gold-2a treatment. The significant effects of gold-2a on *CTNNB1* and *WNT5B* expression were observed from 6 hours of treatment onward. Similar trends of changes were also shown for the protein expressions of WNT1, WNT5B, WIF1, and WISP1 (Fig. 2). These results indicated that gold-2a might elicit its antiproliferative effects through regulating the gene transcriptions of Wnt/β-catenin signaling molecules.

Gold-2a acts as a selective HDAC inhibitor to regulate histone acetylation at the promoter regions of genes involved in Wnt/β-catenin signaling. The above results showed that gold-2a could selectively enhance the gene expression of *WIF1* and noncanonical *WNT5B* but inhibit those of *WNT1, CTNNB1*, and *WISP1*. Epigenetic regulations, such as DNA methylation and histone acetylation, represent important mechanisms for the aberrant activation of Wnt signaling during cancer development. The results in Fig. 3 showed that gold-2a exhibited potent inhibitory effects on the enzyme activities of HDAC, the dynamic transcriptional regulator for deacetylating chromatin histones. Treatment with gold-2a resulted in a rapid decrease of the HDAC activities in MDA-MB-231 cells (Fig. 3*A*). The inhibitory effects could also be observed by coincubation of gold-2a with the nuclear extracts derived from untreated MDA-MB-231 cells (Fig. 3*B*). The HDAC inhibition was proportional to the incubation time, and the potency of gold-2a was comparable with that of trichostatin A (TSA), a specific inhibitor for multiple HDACs (27, 28). To test whether gold-2a could act as a preferential inhibitor, individual HDAC (HDAC1–HDAC9) was immunoprecipitated from the MDA-MB-231 cells and incubated with gold-2a, which was found to be able to inhibit the activity of all class I HDACs, including HDAC1, HDAC2, HDAC3, and HDAC8 (Fig. 3*C*).

To further confirm these unexpected observations, ChIP-PCR was performed to quantify the acetylated histone H4 levels at the promoter regions of the above genes. As the results shown in Fig. 4, treatment with gold-2a enhanced the binding of acetylated histone H4 to *WIF1* and *WNT5B* promoters. In contrast, a decrease in acetylated histone H4 was observed at *WNT1* promoter after gold-2a treatment. TSA had no significant effects on these three genes but increased acetylated histone H4 binding to the promoter of estrogen receptor α (*ESR1*). The acetylated histone H4 binding to the promoter of β-catenin gene (*CTNNB1*) and *WISP1* was not significantly altered by gold-2a or TSA treatment. Western blotting analysis showed significant induction of histone H4 acetylation by TSA, which occurred as early as 6 hours after treatment (Fig. 4). Gold-2a was less effective on global histone H4 acetylation. Similar levels of acetylated histone H4 were only observed at 24 hours after treatment.

Among the four members of class I HDACs, HDAC2 could not be detected at the promoters of all five Wnt pathway genes, despite that it was present at the promoter of *ESR1*. The abundance of HDAC1, HDAC3, and HDAC8 was highly variable at the promoter regions of these genes (Fig. 5). HDAC1 was more abundantly associated with *WNT5B* than other promoters. HDAC3 was not associated with *WNT5B* promoter. The amounts of HDAC3 and HDAC8 at *WIF1* promoter were much higher than the other four genes. The highest and lowest association could differ by as much as 10,000 times. With this information, the significant fold increases

Published OnlineFirst December 8, 2009; DOI: 10.1158/0008-5472.CAN-09-3324

that were below 10 may not be biologically important. Gold-2a, to a greater extent, elicited inhibitory effects on the associations of different HDACs to the promoters of *WIF1, WNT1, WNT5B*, and *CTNNB1* (Fig. 5). In samples treated with 1 μmol/L gold-2a, HDAC1 at the promoters of *WIF1* and *WNT5B* was dramatically decreased by 54- and 164-fold, respectively; HDAC3 at the promoters of *WIF1, WNT1*, and *CTNNB1* was downregulated by 193-, 23-, and 162-fold, respectively; the binding of HDAC8 to *WIF1* promoter was also found to be downregulated by ~300-fold.

To understand how gold-2a interacts with class I HDAC, molecular docking studies were performed using flexible-ligand docking module of ICM-Pro 3.6-1 based on the known X-ray crystal structures of HDAC8 (Supplementary Fig. S6). As a reference, TSA showed an interaction energy of −10.28 kcal/mol (Supplementary Fig. S6*A* and *C*). The root mean square deviation was within 1.0 Å when compared with the X-ray crystal structure of HDAC8-TSA (PDB code: 1T64). Comparative analysis of the low-energy conformations suggested a strong interaction between gold-2a and the binding pocket at the surface of HDAC8 (binding energy of −9.67 kcal/mol; Supplementary Fig. S6*B* and *D*). Unlike the binding modes of TSA, the side chains of gold-2a are not buried inside the 11-Å channel. The porphyrin rings are filled into the hydrophobic pocket and in close contact (within 4 Å) with amino acid residues Tyr100, Phe152, Gly151, His180, Met274, and Pro273. The OH group of gold-2a points toward the 14-Å internal cavity of HDAC8, which blocks the exit of the 14-Å internal cavity of HDAC8.

Discussion

The presence of nuclear β-catenin in a broad spectrum of human cancers makes Wnt/β-catenin pathway an attractive target for cancer treatment. Nevertheless, the development of such therapeutics is still in its infancy, with no options currently undergoing late-stage clinical trials (29). In breast cancer, the Wnt/β-catenin pathway is mostly deregulated by loss of negative Wnt signaling regulators through epigenetic silencing (30). For example, the Wnt antagonists, such as *WIF1* and secreted frizzled-related protein 1 (*sFRP1*), are inactivated due to promoter hypermethylation (31, 32). The present study showed that the drug complex gold-2a decreased the protein and mRNA levels of β-catenin and inhibited its nuclear transcriptional activities. Whereas the expression of *sFRP1* was extremely low and could not be upregulated by gold-2a, the mRNA levels of *WIF1* were rapidly and dramatically augmented upon drug treatment. On the other hand, the expressions of *WNT1, CTNNB1*, and *WISP1* were abolished by gold-2a. These effects are attributed, at least partly, to the inhibitory actions of gold-2a on class I HDAC activities, which differentially regulate the histone acetylation at the gene promoters of these Wnt signaling molecules. The effects of gold-2a on gene transcription are consistent with its rapid entry into the cell nuclei.

Histone acetylation and deacetylation play fundamental roles in modulating chromatin topology and gene transcription (33). Deacetylation is a process mediated by HDACs, which remove acetyl group from the histone tails,

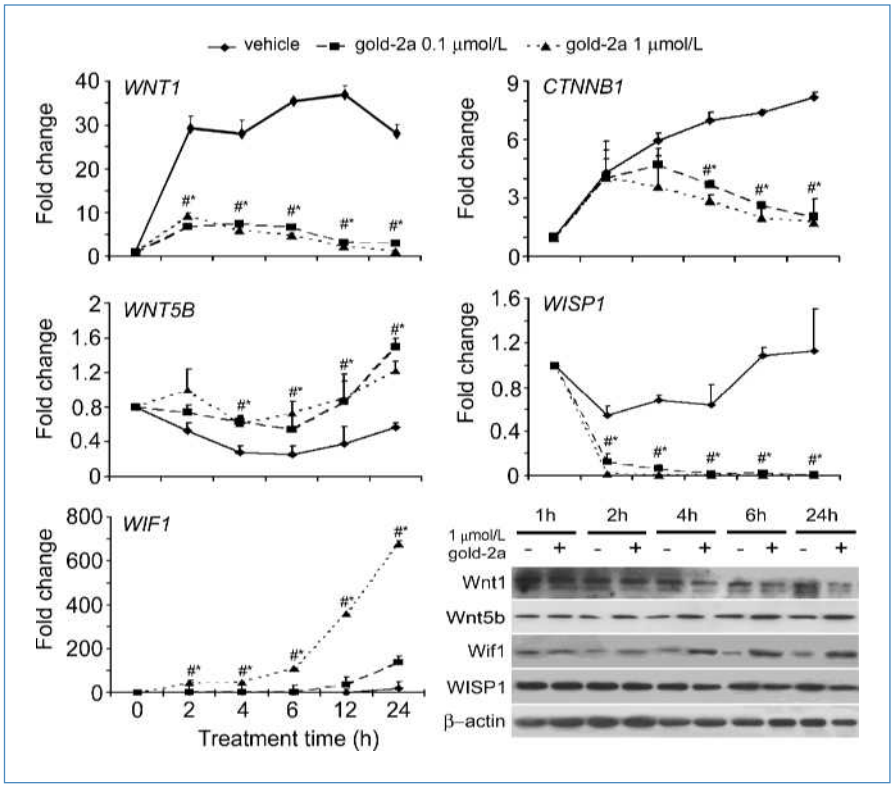

Figure 2. Gold-2a treatment differentially regulates the expression of signaling molecules in Wnt pathway. After 24 h of serum starvation, MDA-MB-231 cells were treated with gold-2a at 0.1 or 1 μmol/L in normal culture media. At different time points, cells were harvested for quantitative RT-PCR analysis. The relative mRNA abundance of *WNT1, WISP1, WNT5B, WIF1*, and *CTNNB1* was normalized against 18S rRNA and calculated as fold changes by comparing to the untreated cells. # and *, $P < 0.05$ for gold-2a treatment at 0.1 and 1 μmol/L, respectively, versus vehicle control ($n = 3$). Western blotting was also performed for evaluating the relative protein abundance of the same set of genes. β-Actin was used as the loading control.

Published OnlineFirst December 8, 2009; DOI: 10.1158/0008-5472.CAN-09-3324

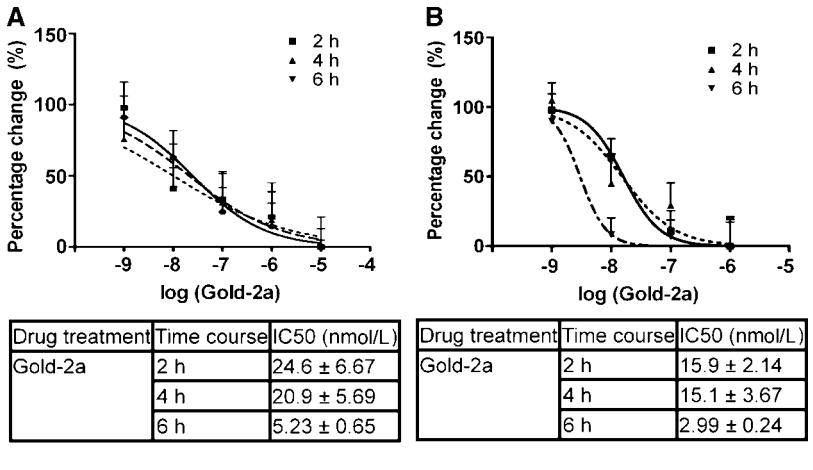

Drug treatment	Time course	IC50 (nmol/L)
Gold-2a	2 h	24.6 ± 6.67
	4 h	20.9 ± 5.69
	6 h	5.23 ± 0.65

Drug treatment	Time course	IC50 (nmol/L)
Gold-2a	2 h	15.9 ± 2.14
	4 h	15.1 ± 3.67
	6 h	2.99 ± 0.24

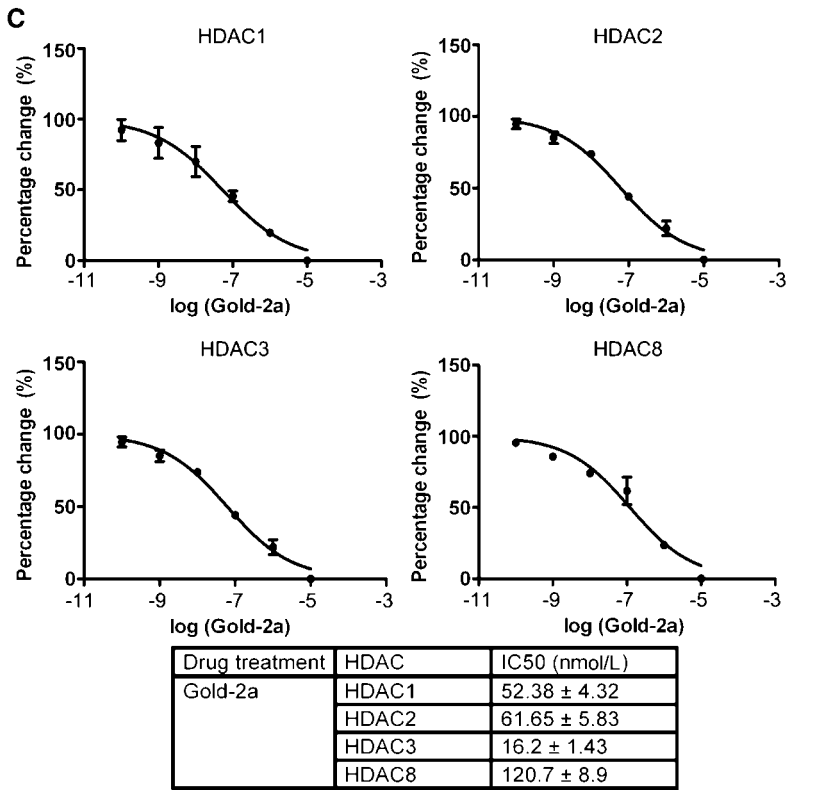

Drug treatment	HDAC	IC50 (nmol/L)
Gold-2a	HDAC1	52.38 ± 4.32
	HDAC2	61.65 ± 5.83
	HDAC3	16.2 ± 1.43
	HDAC8	120.7 ± 8.9

Figure 3. Gold-2a inhibits class I HDAC activities. *A,* MDA-MB-231 cells were treated with different dosages of gold-2a for 2, 4, and 6 h. Nuclear lysates were harvested for HDAC activities measurement. IC_{50} was calculated and listed in Table 1. *B,* nuclear lysates of MDA-MB-231 cells were incubated with gold-2a for different time points, and HDAC activity was measured as above. IC_{50} was calculated and listed in Table 1. *C,* the immunoprecipitated complexes of HDAC1, HDAC2, HDAC3, and HDAC8 were incubated with different concentrations of gold-2a for 1 h, and the HDAC activities were measured at the end of treatment. $n = 4$, results were from three independent assays.

causing the histones to wrap more tightly around the DNA and interfere with gene transcriptions. HDACs are often overexpressed in tumors compared with surrounding normal tissue and correlated with poor prognosis and survival rate (34). HDAC inhibitors (HDACi) are a promising new class of anticancer agents that can inhibit proliferation and induce differentiation and/or apoptosis of tumor cells, with little toxicity to normal cells (35, 36). Several HDACis are currently in phases I and II clinical trials on hematologic and solid malignancies (37–39). Results in the present study suggested gold-2a to be a potential HDACi. It dose- and time-dependently inhibited the HDAC activities in both cell cultures and isolated nuclear extracts and also regulated the global histone acetylation levels, despite of a lower efficiency than TSA. Although the overall result of deacetylation is a global (nonspecific) reduction in gene expression, it has been found that HDACi can selectively modulate a certain set of genes (36, 40). Here, the results showed that gold-2a regulated promoter histone acetylation in a different manner from that of TSA. Gold-2a was more effective on Wnt/β-catenin signaling genes but had less effect on *ESR1*. Although the detailed mechanisms

Published OnlineFirst December 8, 2009; DOI: 10.1158/0008-5472.CAN-09-3324

underlying the HDACi effects of gold-2a were not fully addressed in the present study, experiments using individual immunoprecipitated HDAC complexes revealed that this drug complex might act as a preferential inhibitor for class I HDACs. The proposed mechanism of gold-2a as a class I HDACi was further supported by molecular modeling of the binding interactions with HDAC8 (with favorable calculated binding energy of −9.67 kcal/mol). Although the three-dimensional structures of all HDACs have not been fully resolved, the available evidence suggest that the hydrophobic pockets on their surface near the exit of the 14-Å channel show the most flexibility comparing with other regions (41). Gold-2a occupies almost all pockets of HDAC8 and blocks the entry of the 11-Å channel and the exit of the 14-Å internal cavity. On the other hand, TSA interacts with only one of these pockets. The bulk structure of gold-2a may allow stronger but more selective interactions with certain types of HDACs. Our unpublished data suggested that gold-2a may share similar mechanisms with cyclic tetrapeptide, a distinct class of HDACi (42).

Comparing with cisplatin, which had no effect on both protein stabilities and nuclear activities of β-catenin, gold-2a showed more potent cytotoxic effects in cell culture and better anticancer activities in nude mice with less systematic toxicity. The antiproliferative activities of gold-2a in MDA-MB-231 cells were comparable with other HDACi, such as SAHA (43) and TSA (44). Previous studies have suggested that cisplatin and gold (III) porphyrin complexes elicit their anticancer effects through distinct mechanisms at the DNA level and the protein level, respectively (45–48). Among the five types of human breast cancer cells, MDA-MB-231 possesses the most active autocrine canonical Wnt signaling, followed by SKBR3, T47D, MCF-7, and BT474 (16, 49), indicating that gold-2a may favor on targeting cancers that are more addicted to Wnt/β-catenin signaling. We have previously reported that

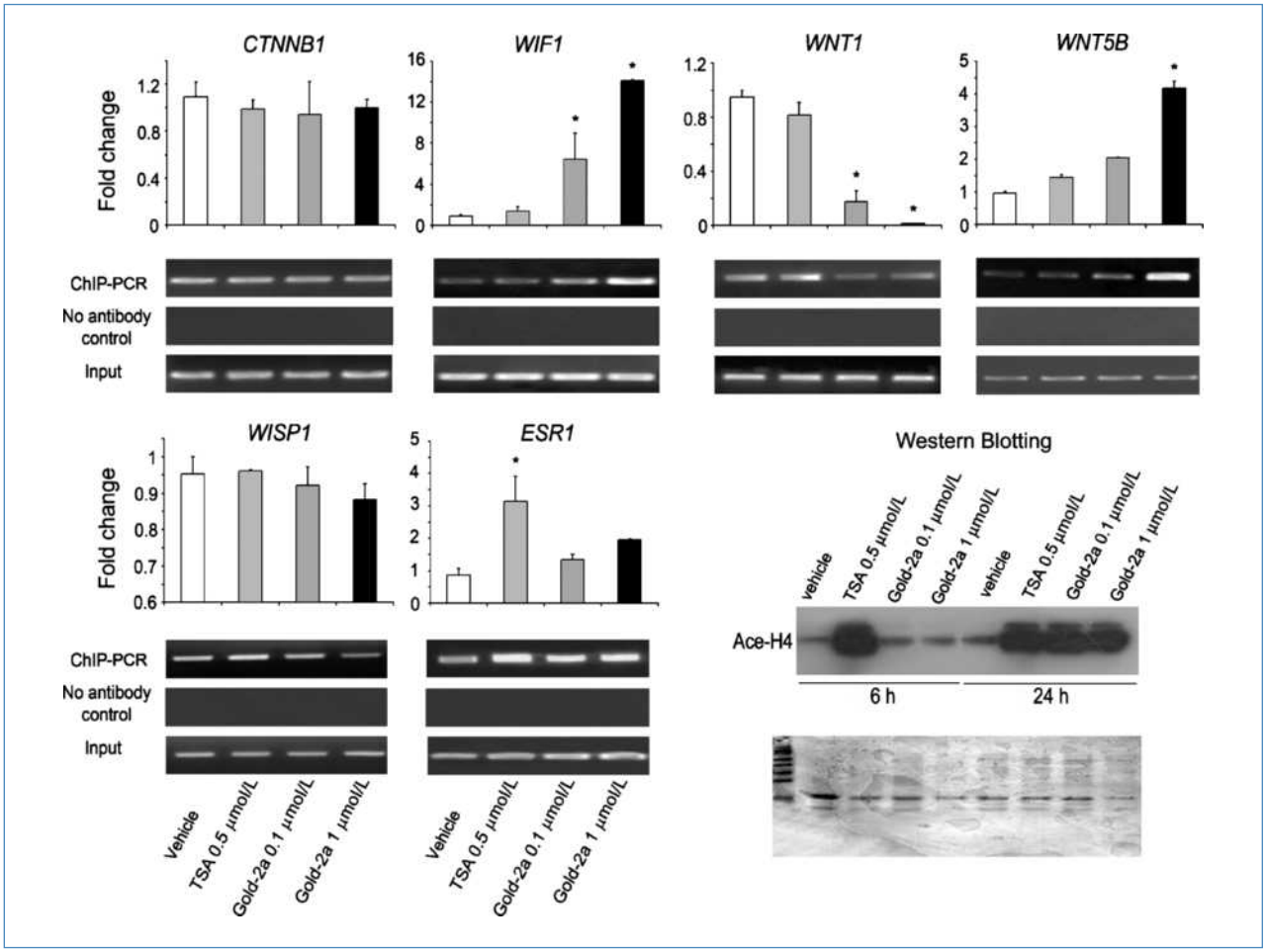

Figure 4. Gold-2a modulates the acetylation status of histone H4 at the promoter regions of Wnt signaling molecules. MDA-MB-231 cells were treated with different drugs for 24 h. ChIP-PCR was performed for analyzing the levels of acetylated histone H4 at the promoter regions of *CTNNB1, WIF1, WNT5B, WNT1, WISP1*, and *ESR1* (active gene control), using antibody recognizing histone H4 acetylated at lysines 5, 8, 12, and 16. Bar charts represent the quantitative results by real-time PCR analysis after normalization against the input DNA. Representative agarose gel images are shown at the bottom. Western blotting was performed for analyzing the global acetylated histone H4 (*Ace-H4*) levels in MDA-MB-231 cells treated with TSA or gold-2a for 6 and 24 h, respectively. Equal protein loading was confirmed by Ponceau S staining. *, $P < 0.01$ versus vehicle control ($n = 3$).

Published OnlineFirst December 8, 2009; DOI: 10.1158/0008-5472.CAN-09-3324

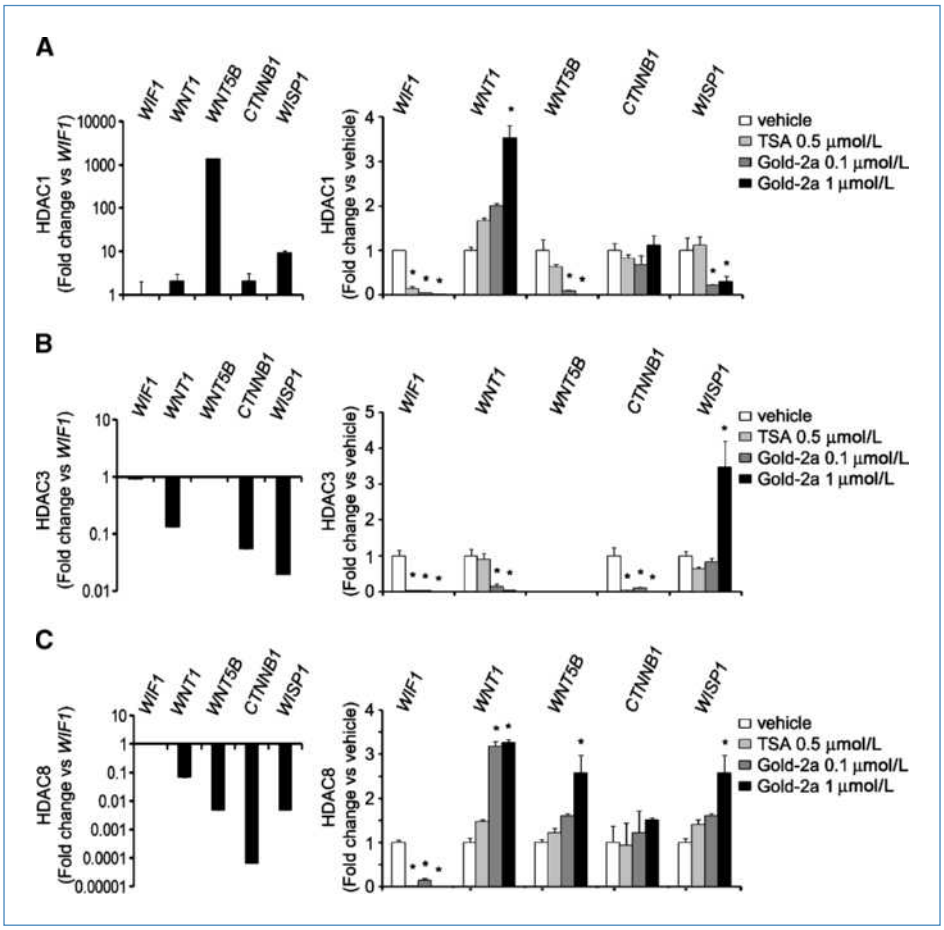

Figure 5. Gold-2a differentially regulates the associations of class I HDACs to the promoter regions of the five Wnt signaling molecules. ChIP-PCR was performed using MDA-MB-231 cells that had been treated with or without drug compounds at the indicated concentrations for 24 h. The associations of HDAC1 (*A*), HDAC3 (*B*), and HDAC8 (*C*) were quantified by real-time PCR analysis. *Left,* the amount of each HDAC bound to the promoter regions of individual gene was compared and calculated as fold change versus *WIF1* to reflect their relative abundances. The *y* axis is at logarithmic scale. *Right,* the associations of HDAC1, HDAC3, or HDAC8 to the promoters of *WIF1, WNT1, WNT5B, CTNNB1*, and *WISP1* were quantified and calculated against vehicle control samples. *, $P < 0.01$ ($n = 3$).

gold(III) porphyrin 1a (gold-1a) can induce apoptosis through both caspase-dependent and caspase-independent mitochondrial pathways (14). The results from the present study suggest that the two compounds, although possessing similar chemical structures, might not share common cytotoxic mechanisms at the molecular level. The difference between gold-1a and gold-2a is the replacement of a benzene group by a phenol group. Subha and colleagues have reported that the presence of hydroxyl groups on test inhibitor compounds can favor the fitting into the active site of HDAC (50). It remains to be addressed whether the presence of a hydroxyl group in gold-2a assists this compound in targeting HDACs and whether the presence of more hydroxyl groups at the side arms of these gold(III) porphyrins contributes to higher toxicity or more potent inhibition toward HDACs. Further investigations are currently being carried out in our laboratory for elucidating the detailed mechanisms contributing to the selective inhibitory activities of gold-2a on HDACs.

Disclosure of Potential Conflicts of Interest

No potential conflicts of interest were disclosed.

Grant Support

Grants from Seeding Funds for Basic Research of the University of Hong Kong (Y. Wang), Hong Kong Research Grant Council grants HKU 777908M (Y. Wang) and HKU 779707M (A. Xu), and the Area of Excellent Scheme AoE/P-10-01 established under University Grants Committee HKSAR (C. Che).

The costs of publication of this article were defrayed in part by the payment of page charges. This article must therefore be hereby marked *advertisement* in accordance with 18 U.S.C. Section 1734 solely to indicate this fact.

Received 9/8/09; revised 10/21/09; accepted 10/23/09; published OnlineFirst 12/8/09.

References

1. American Cancer Society. Breast cancer facts and figures 2007–2008. Atlanta: American Cancer Society, Inc.; 2007.
2. Buzdar AU. Role of biologic therapy and chemotherapy in hormone receptor- and HER2-positive breast cancer. Ann Oncol 2009;20:993–9.
3. Shaw CFI. Gold-based therapeutic agents. Chem Rev 1999;99:2589–600.
4. Sun RW, Ma DL, Wong EL, Che CM. Some uses of transition metal complexes as anti-cancer and anti-HIV agents. Dalton Trans 2007;43:4884–92.

5. Zhang CX, Lippard SJ. New metal complexes as potential therapeutics. Curr Opin Chem Biol 2003;7:481–9.
6. Bruijnincx PC, Sadler PJ. New trends for metal complexes with anticancer activity. Curr Opin Chem Biol 2008;12:197–206.
7. Milacic V, Fregona D, Dou QP. Gold complexes as prospective metal-based anticancer drugs. Histol Histopathol 2008;23:101–8.
8. Chen D, Milacic V, Frezza M, Dou QP. Metal complexes, their cellular targets and potential for cancer therapy. Curr Pharm Des 2009;15:777–91.
9. Nobili S, Mini E, Landini I, Gabbiani C, Casini A, Messori L. Gold compounds as anticancer agents: chemistry, cellular pharmacology, and preclinical studies. Med Res Rev. Epub 2009 Jul 24.
10. Casini A, Hartinger C, Gabbiani C, et al. Gold(III) compounds as anticancer agents: relevance of gold-protein interactions for their mechanism of action. J Inorg Biochem 2008;102:564–75.
11. Che CM, Sun RW, Yu WY, Ko CB, Zhu N, Sun H. Gold(III) porphyrins as a new class of anticancer drugs: cytotoxicity, DNA binding and induction of apoptosis in human cervix epitheloid cancer cells. Chem Commun (Camb) 2003;14:1718–9.
12. Lum CT, Yang ZF, Li HY, et al. Gold(III) compound is a novel chemocytotoxic agent for hepatocellular carcinoma. Int J Cancer 2006;118:1527–38.
13. Wang Y, He QY, Che CM, Tsao SW, Sun RW, Chiu JF. Modulation of gold(III) porphyrin 1a-induced apoptosis by mitogen-activated protein kinase signaling pathways. Biochem Pharmacol 2008;75:1282–91.
14. Wang Y, He QY, Sun RW, Che CM, Chiu JF. Gold(III) porphyrin 1a induced apoptosis by mitochondrial death pathways related to reactive oxygen species. Cancer Res 2005;65:11553–64.
15. Wang Y, He QY, Sun RW, Che CM, Chiu JF. Cellular pharmacological properties of gold(III) porphyrin 1a, a potential anticancer drug lead. Eur J Pharmacol 2007;554:113–22.
16. Liu J, Lam JB, Chow KH, et al. Adiponectin stimulates Wnt inhibitory factor-1 expression through epigenetic regulations involving the transcription factor specificity protein 1. Carcinogenesis 2008;29:2195–202.
17. Wang Y, Lam JB, Lam KS, et al. Adiponectin modulates the glycogen synthase kinase-3β/β-catenin signaling pathway and attenuates mammary tumorigenesis of MDA-MB-231 cells in nude mice. Cancer Res 2006;66:11462–70.
18. Cousens LS, Gallwitz D, Alberts BM. Different accessibilities in chromatin to histone acetylase. J Biol Chem 1979;254:1716–23.
19. Graham JM, Rickwood D. Subcellular fractionation: a practical approach. Oxford: IRL Press; 1997.
20. Kebbekus BB. Preparation of samples for metal analysis. In: Mitra S, editor. Sample preparation techniques in analytical chemistry. Hoboken: John Wiley & Sons, Inc.; 2003. p. 227–64.
21. Hay PJ, Wadt WR. Ab initio effective core potentials for molecular calculations. Potentials for K to Au including the outermost core orbitals. J Chem Phys 1985;82:299.
22. Totrov M, Abagyan R. Flexible protein-ligand docking by global energy optimization in internal coordinates. Proteins 1997;Suppl 1:215–20.
23. Lacroix M, Leclercq G. Relevance of breast cancer cell lines as models for breast tumours: an update. Breast Cancer Res Treat 2004;83:249–89.
24. Huang H, He X. Wnt/β-catenin signaling: new (and old) players and new insights. Curr Opin Cell Biol 2008;20:119–25.
25. Howe LR, Brown AM. Wnt signaling and breast cancer. Cancer Biol Ther 2004;3:36–41.
26. Giarre M, Semenov MV, Brown AM. Wnt signaling stabilizes the dual-function protein β-catenin in diverse cell types. Ann N Y Acad Sci 1998;857:43–55.
27. Glaser KB, Staver MJ, Waring JF, Stender J, Ulrich RG, Davidsen SK. Gene expression profiling of multiple histone deacetylase (HDAC) inhibitors: defining a common gene set produced by HDAC inhibition in T24 and MDA carcinoma cell lines. Mol Cancer Ther 2003;2:151–63.
28. Joung KE, Min KN, An JY, Kim DK, Kong G, Sheen YY. Potent *in vivo* anti-breast cancer activity of IN-2001, a novel inhibitor of histone deacetylase, in MMTV/c-Neu mice. Cancer Res 2006;66:5394–402.
29. Garber K. Drugging the Wnt pathway: problems and progress. J Natl Cancer Inst 2009;101:548–50.
30. Klarmann GJ, Decker A, Farrar WL. Epigenetic gene silencing in the Wnt pathway in breast cancer. Epigenetics 2008;3:59–63.
31. Veeck J, Niederacher D, An H, et al. Aberrant methylation of the Wnt antagonist SFRP1 in breast cancer is associated with unfavourable prognosis. Oncogene 2006;25:3479–88.
32. Ai L, Tao Q, Zhong S, et al. Inactivation of Wnt inhibitory factor-1 (WIF1) expression by epigenetic silencing is a common event in breast cancer. Carcinogenesis 2006;27:1341–8.
33. Demeret C, Vassetzky Y, Mechali M. Chromatin remodelling and DNA replication: from nucleosomes to loop domains. Oncogene 2001;20:3086–93.
34. Weichert W. HDAC expression and clinical prognosis in human malignancies. Cancer Lett 2009;280:168–76.
35. Marks PA, Richon VM, Breslow R, Rifkind RA. Histone deacetylase inhibitors as new cancer drugs. Curr Opin Oncol 2001;13:477–83.
36. Klampfer L, Huang J, Shirasawa S, Sasazuki T, Augenlicht L. Histone deacetylase inhibitors induce cell death selectively in cells that harbor activated kRasV12: the role of signal transducers and activators of transcription 1 and p21. Cancer Res 2007;67:8477–85.
37. Bolden JE, Peart MJ, Johnstone RW. Anticancer activities of histone deacetylase inhibitors. Nat Rev Drug Discov 2006;5:769–84.
38. Minucci S, Pelicci PG. Histone deacetylase inhibitors and the promise of epigenetic (and more) treatments for cancer. Nat Rev Cancer 2006;6:38–51.
39. Yang XJ, Seto E. HATs and HDACs: from structure, function and regulation to novel strategies for therapy and prevention. Oncogene 2007;26:5310–8.
40. Johnstone RW, Licht JD. Histone deacetylase inhibitors in cancer therapy: is transcription the primary target? Cancer Cell 2003;4:13–8.
41. Wang DF, Wiest O, Helquist P, Lan-Hargest HY, Wiech NL. On the function of the 14 A long internal cavity of histone deacetylase-like protein: implications for the design of histone deacetylase inhibitors. J Med Chem 2004;47:3409–17.
42. Montero A, Beierle JM, Olsen CA, Ghadiri MR. Design, synthesis, biological evaluation, and structural characterization of potent histone deacetylase inhibitors based on cyclic α/β-tetrapeptide architectures. J Am Chem Soc 2009;131:3033–41.
43. Price S, Bordogna W, Braganza R, et al. Identification and optimisation of a series of substituted 5-pyridin-2-yl-thiophene-2-hydroxamic acids as potent histone deacetylase (HDAC) inhibitors. Bioorg Med Chem Lett 2007;17:363–9.
44. Vigushin DM, Ali S, Pace PE, et al. Trichostatin A is a histone deacetylase inhibitor with potent antitumor activity against breast cancer *in vivo*. Clin Cancer Res 2001;7:971–6.
45. Coronnello M, Mini E, Caciagli B, et al. Mechanisms of cytotoxicity of selected organogold(III) compounds. J Med Chem 2005;48:6761–5.
46. Milacic V, Chen D, Ronconi L, Landis-Piwowar KR, Fregona D, Dou QP. A novel anticancer gold(III) dithiocarbamate compound inhibits the activity of a purified 20S proteasome and 26S proteasome in human breast cancer cell cultures and xenografts. Cancer Res 2006;66:10478–86.
47. Saggioro D, Rigobello MP, Paloschi L, et al. Gold(III)-dithiocarbamato complexes induce cancer cell death triggered by thioredoxin redox system inhibition and activation of ERK pathway. Chem Biol 2007;14:1128–39.
48. To YF, Sun RW, Chen Y, et al. Gold(III) porphyrin complex is more potent than cisplatin in inhibiting growth of nasopharyngeal carcinoma *in vitro* and *in vivo*. Int J Cancer 2009;124:1971–9.
49. Schlange T, Matsuda Y, Lienhard S, Huber A, Hynes NE. Autocrine WNT signaling contributes to breast cancer cell proliferation via the canonical WNT pathway and EGFR transactivation. Breast Cancer Res 2007;9:R63.
50. Subha K, Kumar GR. Assessment for the identification of better HDAC inhibitor class through binding energy calculations and descriptor analysis. Bioinformation 2008;3:218–22.

Published OnlineFirst December 8, 2009; DOI: 10.1158/0008-5472.CAN-09-3324

AACR American Association for Cancer Research

Cancer Research

The Journal of Cancer Research (1916–1930) | The American Journal of Cancer (1931–1940)

A Gold(III) Porphyrin Complex with Antitumor Properties Targets the Wnt/ β-catenin Pathway

Kim Hei-Man Chow, Raymond Wai-Yin Sun, Janice B.B. Lam, et al.

Cancer Res 2010;70:329-337. Published OnlineFirst December 8, 2009.